

Comparative study of autofluorescence in flat and tapered optical fibers towards application in depth-resolved fluorescence lifetime photometry in brain tissue: supplement

MARCO BIANCO,^{1,2,*}  ANTONIO BALENA,^{1,2}  MARCO PISANELLO,¹  FILIPPO PISANO,¹  LEONARDO SILEO,¹ BARBARA SPAGNOLO,¹ CINZIA MONTINARO,^{1,3} BERNARDO L. SABATINI,⁴ MASSIMO DE VITTORIO,^{1,2,5} AND FERRUCCIO PISANELLO^{1,6} 

¹*Istituto Italiano di Tecnologia (IIT), Center for Biomolecular Nanotechnologies, Via Barsanti 14, 73010 Arnesano (Lecce), Italy*

²*Dipartimento di Ingegneria dell'Innovazione, Università del Salento, Via per Monteroni, 73100 Lecce, Italy*

³*Dipartimento di Scienze e Tecnologie Biologiche e Ambientali, Università del Salento, Via per Monteroni, 73100 Lecce, Italy*

⁴*Howard Hughes Medical Institute, Department of Neurobiology, Harvard Medical School, Boston, MA 02115, USA*

⁵*massimo.devittorio@iit.it*

⁶*ferruccio.pisanello@iit.it*

**marco.bianco@iit.it*

This supplement published with The Optical Society on 26 January 2021 by The Authors under the terms of the [Creative Commons Attribution 4.0 License](https://creativecommons.org/licenses/by/4.0/) in the format provided by the authors and unedited. Further distribution of this work must maintain attribution to the author(s) and the published article's title, journal citation, and DOI.

Supplement DOI: <https://doi.org/10.6084/m9.figshare.13499202>

Parent Article DOI: <https://doi.org/10.1364/BOE.410244>

Comparative study of autofluorescence in flat and tapered optical fibers towards application in depth-resolved fluorescence lifetime photometry in brain tissue

MARCO BIANCO^{1,2,*}, ANTONIO BALENA^{1,2}, MARCO PISANELLO¹, FILIPPO PISANO¹, LEONARDO SILEO¹, BARBARA SPAGNOLO¹, CINZIA MONTINARO^{1,3}, BERNARDO L. SABATINI⁴, MASSIMO DE VITTORIO^{1,2,5}, FERRUCCIO PISANELLO^{1,5}

¹*Istituto Italiano di Tecnologia (IIT), Center for Biomolecular Nanotechnologies, Via Barsanti 14, 73010 Arnesano (Lecce), Italy*

²*Dipartimento di Ingegneria dell'Innovazione, Università del Salento, Via per Monteroni, 73100 Lecce, Italy*

³*Dipartimento di Scienze e Tecnologie Biologiche e Ambientali, Università del Salento, Via per Monteroni, 73100 Lecce, Italy*

⁴*Department of Neurobiology, Howard Hughes Medical Institute, Harvard Medical School, Boston, MA, 02115*

⁵ massimo.devittorio@iit.it

⁶ ferruccio.pisanello@iit.it

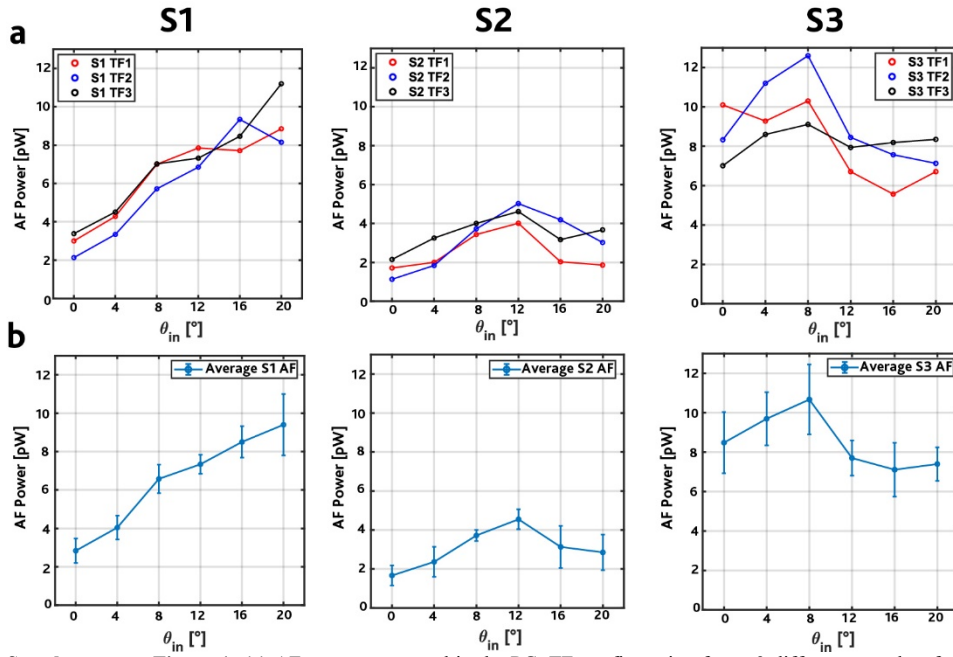
* marco.bianco@iit.it

© 2020 Optical Society of America

Supplementary Material

1. Supplementary Figure 1

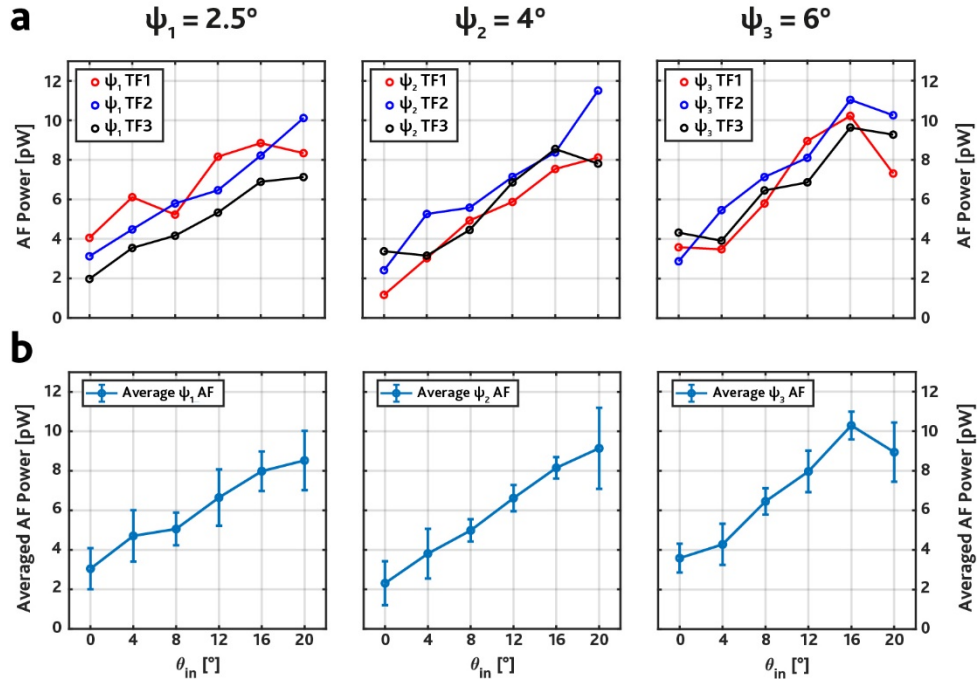
We performed AF measurements for $n=3$ S1, $n=3$ S2 and $n=3$ S3 TF probes. The results of the measurements are shown in *Supplementary Figure 1a*. *Supplementary Figure 1b* shows the mean and standard deviation of the data for every type of sample.



Supplementary Figure 1: (a) AF power measured in the PC+TF configuration for $n=3$ different samples, for every fiber type, as a function of θ_{in} . (b) Mean and standard deviation of the data in panels (a).

2. Supplementary Figure 2

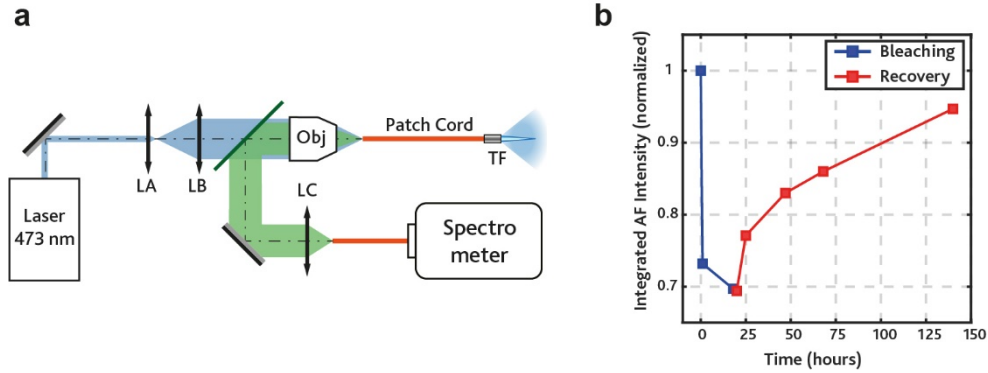
We performed a more detailed analysis for sample S1, acquiring AF intensity as a function of θ_{in} for $n=3$ samples taper angles: $\psi_1 = 2.5^\circ$ ($n=3$), $\psi_2 = 4^\circ$ ($n=3$), $\psi_3 = 6^\circ$ ($n=3$). Data are reported in *Supplementary Figure 2*, both for single measurements (*Supplementary Figure 2a*), and in terms of mean and standard deviation (*Supplementary Figure 2b*). It is possible to see that the AF power tend to increase as a function of θ_{in} for all the taper angles investigated, with no major differences as function of θ_{in} .



Supplementary Figure 2: AF measurement as a function of θ_{in} for S1 TFs with different taper angles. (a) shows data on $n=3$ different TFs for each tested ψ , (b) shows their mean value and standard deviation (error bars).

3. Supplementary Figure 3

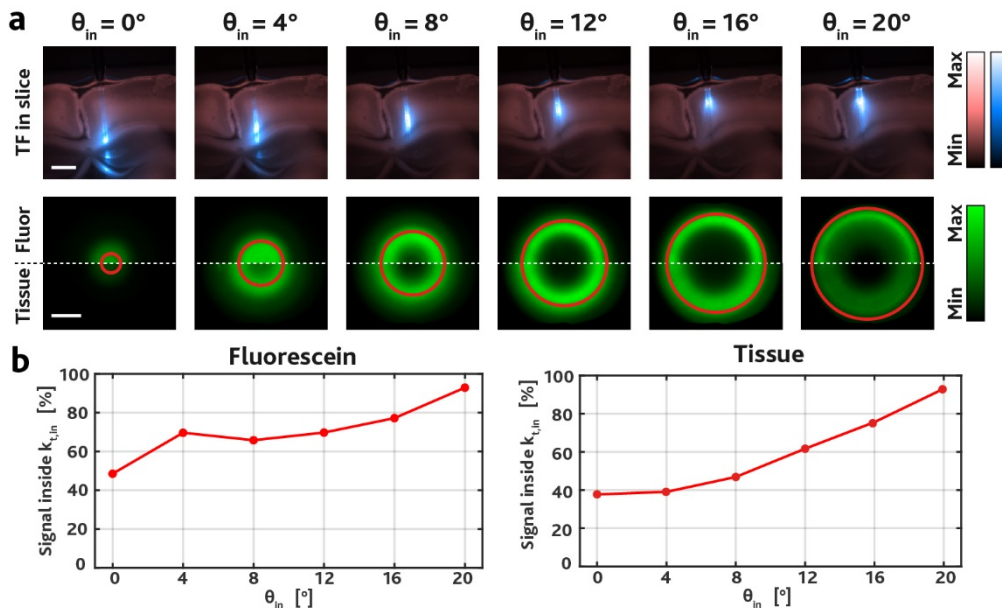
We have performed the photobleaching of a patch cord with a S1 TF connected to its end, using a full-NA injection of a 473 nm laser beam. The power injected in the patch cord was set at 50 mW and autofluorescence was collected and sent to a spectrometer. The device was photobleached for 24 hours and the recovery followed over several days. Spectra were acquired and integrated in the range from 500 nm to 550 nm, resulting in the data displayed in *Supplementary Figure 3*. AF was reduced in the first hour of photobleaching, and continued to decrease during the next 23h, stabilising at 70% of the initial value. AF recovery after 1 day of photobleaching was instead slower, with the overall intensity increasing from 70% to 95% of the initial value in 4 days. Therefore photobleaching could be a good treatment to partially reduce the AF generated both by the patch cord and by the TF.



Supplementary Figure 3: (a) Setup used for the photobleaching process. Lenses LA ($f_A = 15 \text{ mm}$) and LB ($f_B = 100 \text{ mm}$) act as a beam expander (BE) in order to fill the back focal plane of the objective (Obj), which focuses the light in the patch cord. AF is back-propagated and focused in a spectrometer using LC ($f_C = 100 \text{ mm}$). (b) Graph showing the integrated intensity of the AF spectra normalized to the maximum value as a function of time. Blue line represents the bleaching process, red line represents the recovery phase.

4. Supplementary Figure 4

We have performed far-field acquisition with both the TF in PBS:fluorescein and the TF inserted in a scattering brain slice. Data are reported in *Supplementary Figure 4*. In the top row of panel (a) brightfield images (pink) show that the fiber is inserted in a region extending from the cortex to the hippocampus. Fluorescence images (blue) are overlaid to show the different emitting region as a function of the input angle. Bottom row displays instead the acquired far-field pattern for the corresponding emitting position, both in a $30 \mu\text{M}$ PBS:fluorescein solution (as a reference for non-dispersive medium) and in the brain slice. It can be observed that the distribution of light is similar in both cases, albeit acquired data in tissue show a broader profile.

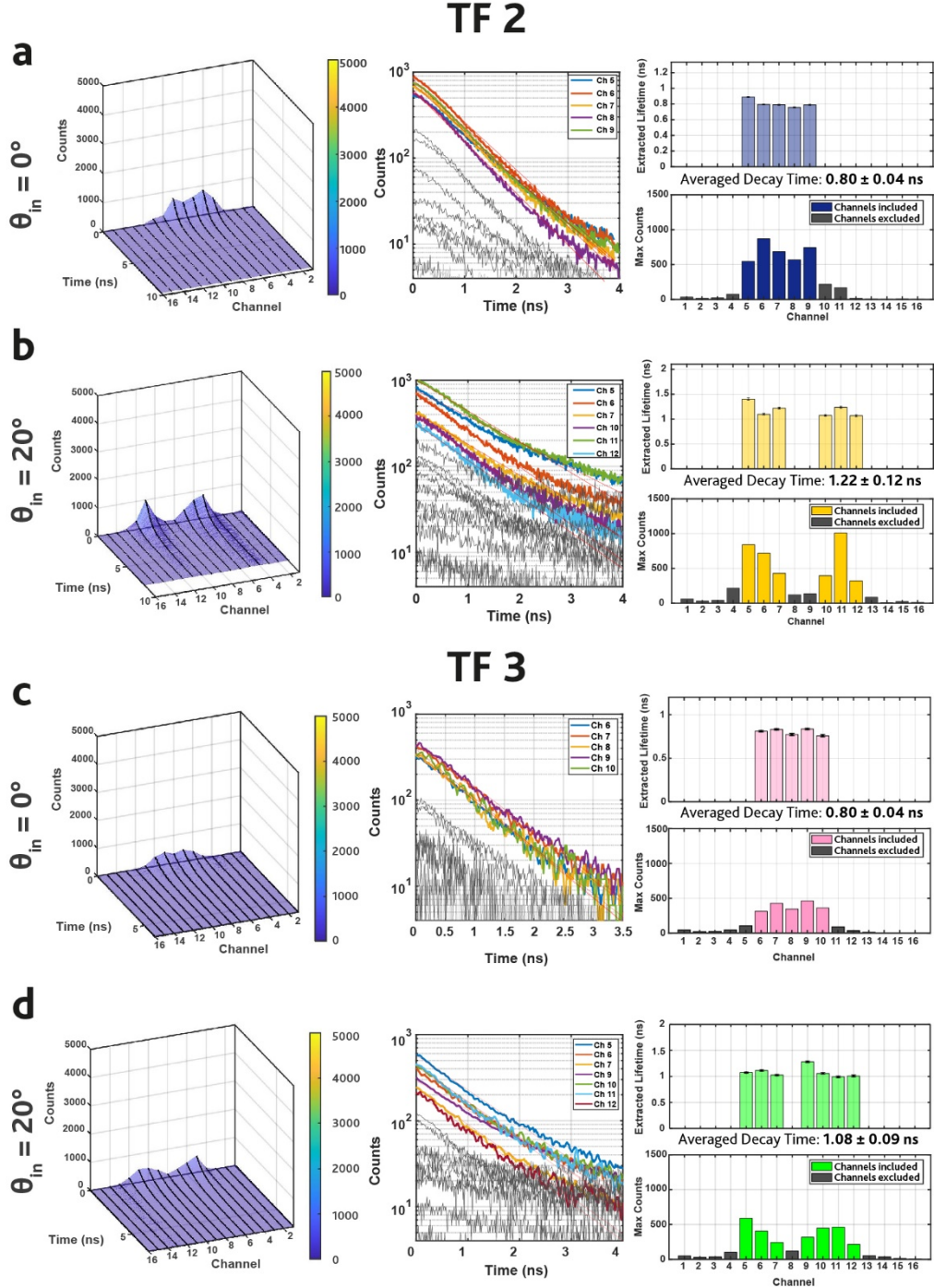


Supplementary Figure 4: (a) Top row: Fluorescence images of the TF inserted in a brain slice of a (Thy1-

GCaMP6s) GP4.12Dkim/J mouse, showing different emitting position as a function of θ_{in} . Scale bar represents 500 μm . Bottom row: Acquired far-field pattern for the corresponding emitting position, both in PBS:fluorescein solution, and in brain tissue. Scale bar represents $0.2 \cdot 2\pi/\lambda$. Red circle represents $\mathbf{k}_{t,in}$ (b) Plots of the percentage of $\mathbf{k}_{t,fluor} \leq \mathbf{k}_{t,in}$ both in fluorescein and in tissue.

5. Supplementary Figure 5

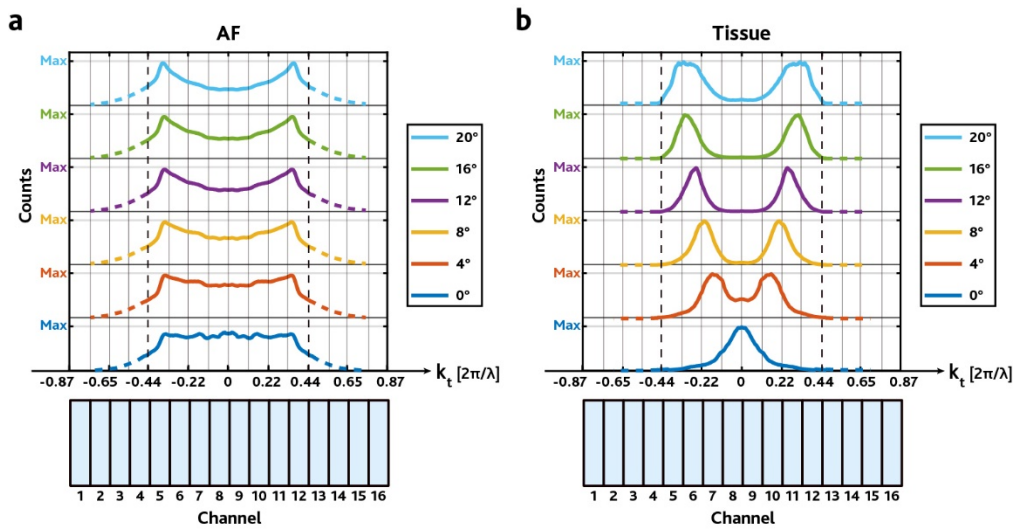
Additional AF decay curves acquired with S2 TFs in air. The extracted lifetimes are compatible with those reported in *Figure 5*. With the lifetimes reported in *Supplementary Figure 5* and in *Figure 5* in the manuscript, it is possible to evaluate mean and standard deviation for the lifetime of the AF for a given θ_{in} . We obtain: $\tau_{AF,0^\circ} = 0.82 \pm 0.03 \text{ ns}$ for $\theta_{in} = 0^\circ$, and $\tau_{AF,20^\circ} = 1.16 \pm 0.10 \text{ ns}$ for $\theta_{in} = 20^\circ$.



Supplementary Figure 5: (a-b) Representative DR-FLiP data extracted from a S2 probe in air (TF2), $\theta_{in} = 0^\circ$ (a) and $\theta_{in} = 20^\circ$ (b). Left column is the decay map for all the channels of the array. Center column shows the results of the fitting for the decay tracks over threshold, logarithmic scale. Tracks under threshold are shown in grey, and are excluded from the evaluation of the lifetime τ . On right column are reported the extracted lifetimes, and the maximum counts per channel. (c-d) Same analysis for another S2 probe in air (TF3), $\theta_{in} = 0^\circ$ (c) and $\theta_{in} = 20^\circ$ (d). It is possible to see that the extracted lifetimes are compatible with the values showed in Figure 5 in the manuscript.

6. Supplementary Figure 6

The far-field light pattern over the PMT channels for different θ_{in} values, both for AF signal (Supplementary Figure 6a), and signal collected in tissue (Supplementary Figure 6b), can be estimated by projecting the far-field pattern profiles acquired with the sCMOS camera on the linear array (calibrated in units of $2\pi/\lambda$). This gives an overview of how this type of detection behaves as a function of the input angle.



Supplementary Figure 6: (a) Normalized profiles extracted from AF far-field images for different θ_{in} projected over the PMT array. According to Equation 2 in the main text, each channel detects a specific range of k_t (using a far-field lens L6 with $f_6 = 35 \text{ mm}$). (b) Normalized far-field profiles acquired with the TF in the mouse brain slice for different θ_{in} .